

ARBITRARILY POLARIZED PLANE-WAVE DIFFRACTION FROM SEMI-INFINITE PERIODIC GROOVES AND ITS APPLICATION TO FINITE PERIODIC GROOVES

Y. H. Cho [†]

Department of Electrical and Computer Engineering
University of Massachusetts Amherst
228 Marcus Hall, University of Massachusetts,
100 Natural Resources Road, Amherst, MA 01003, USA

Abstract—Arbitrarily polarized plane-wave diffraction equations for semi-infinite periodic rectangular grooves (RG) in a perfectly conducting plane are approximately proposed. To obtain diffraction equations for semi-infinite periodic RG, we utilize an overlapping T-block method as proposed for the analyses of finite and infinite numbers of RG, and the subtraction technique with infinite periodic solutions. The proposed semi-infinite solutions are then applied to finite periodic RG with very large number of diffracting elements. For verification of our approach, we performed numerical computations for finite periodic RG and compared our solutions based on semi-infinite equations with previously published analytic solutions, thus obtaining favorable agreement and proving computational efficiency.

1. INTRODUCTION

Periodic gratings are widely used to control electromagnetic field distributions such as optical disks, interferometers, diffraction gratings, non-destructive crack detectors, and solar cells [1–4]. Rectangular metallic grooves (RG) in a conducting plane can constitute diffracting periodic gratings and they are well discussed in [4–7]. The problem of a semi-infinite array with various diffracting elements has been also analyzed with several numerical techniques [7–17]. The diffraction characteristics of periodic gratings are mainly analyzed with periodic

Received 1 March 2011, Accepted 11 April 2011, Scheduled 13 April 2011

Corresponding author: Yong Heui Cho (yongheuicho@gmail.com).

[†] Also on sabbatical leave from School of Information and Communication Engineering, Mokwon University, Korea.

boundary conditions based on the Floquet theorem and modes, even though actual gratings have finite width and their solutions are incorrect near the edges of gratings [1, 2]. Since a semi-infinite array has edge effect on one side, the analysis of a semi-infinite array enables us to understand the diffraction characteristics of a finite periodic array [13]. Thus, it is of theoretical and practical interest to obtain the solutions for the semi-infinite array and extend them to the problem of real diffraction gratings.

In this work, we adopt and extend the same method proposed in [6, 7] to obtain arbitrarily polarized plane-wave solutions for semi-infinite periodic RG. To accelerate the convergence of summations of electromagnetic fields diffracted from each RG, we subtract original fields with infinite periodic ones and constitute the simultaneous equations which are numerically computable. The subtraction technique in [6, 7] was already proposed for acoustic wave scattering [8, 9]. Recently, the analysis method in [8, 9] has been extended to the problem of semi-infinite metal-nanoparticle chains [10].

In the next step, we will judiciously combine the diffracted fields and phases of semi-infinite periodic RG and approximately predict the diffraction behaviors of very large number of finite periodic RG without the loss of precision. In addition to the subtraction technique, the extended Wiener-Hopf factorization technique [11, 14] and a domain reduction technique [12] were proposed to understand the diffraction and coupling effects of semi-infinite arrays. Using the Poisson summation formula [15] and the Floquet waves [16, 17], the Green's functions of a semi-infinite array have been also obtained.

2. SEMI-INFINITE PERIODIC GROOVES

Assume that an arbitrarily polarized plane-wave impinges on semi-infinite periodic RG in a perfectly conducting plane illustrated in Figure 1. The semi-infinite periodicity means that the structure is periodic in only one direction but not both. Each RG in Figure 1 has identical structure and parameters. The time factor $e^{-i\omega t}$ is suppressed throughout. The incident and reflected electric fields are written as

$$\bar{E}^i(x, y) = [u_i (\cos \theta_i \hat{x} + \sin \theta_i \hat{y}) + v_i \hat{z}] \exp [ik_2 (\sin \theta_i x - \cos \theta_i y)] \quad (1)$$

$$\bar{E}^r(x, y) = [u_i (-\cos \theta_i \hat{x} + \sin \theta_i \hat{y}) - v_i \hat{z}] \exp [ik_2 (\sin \theta_i x + \cos \theta_i y)], \quad (2)$$

where $k_{1,2} = \omega \sqrt{\mu_{1,2} \varepsilon_{1,2}}$, u_i and v_i are constants representing the polarization type, and θ_i is an incident angle of the plane-wave. To obtain the diffracted fields from semi-infinite periodic RG $\bar{E}^{tot}(x, y)$, we systematically represent the scattered electric fields for regions (I) ($y < 0$) and (II) ($y > 0$) based on the superposition of overlapping

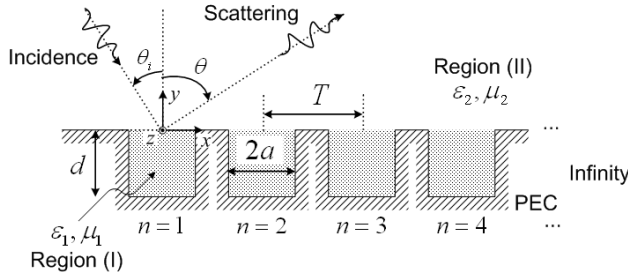


Figure 1. Geometry of semi-infinite periodic rectangular metallic grooves in a perfectly conducting plane.

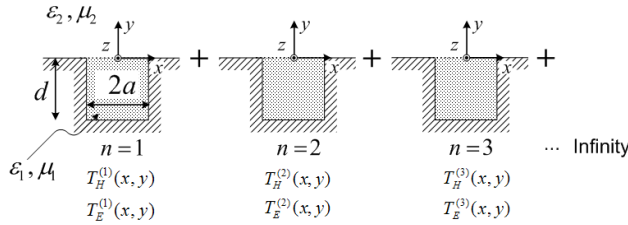


Figure 2. Divided geometry of semi-infinite periodic rectangular metallic grooves based on superposition principle.

T-blocks [6, 7] shown in Figure 2. Superposing and translating a single RG on the PEC plane in Figure 2 from $n = 1$ to $n = \infty$ yields the same geometry of Figure 1. By matching the appropriate boundary conditions, we can determine all fields in Figure 1. Then, we represent the total diffracted fields as

$$\bar{E}^{tot}(x, y) = \hat{\phi}u_i\eta_2 \sum_{n=1}^{\infty} T_H^{(n)}[x-(n-1)T, y] + \hat{z}v_i \sum_{n=1}^{\infty} T_E^{(n)}[x-(n-1)T, y], \quad (3)$$

where $\eta_2 = \sqrt{\mu_2/\epsilon_2}$, $a_m = m\pi/(2a)$, $\xi_m = \sqrt{k_1^2 - a_m^2}$, $\eta_m = \sqrt{k_2^2 - a_m^2}$,

$$T_H^{(n)}(x, y) = \begin{cases} \sum_{m=0}^{\infty} q_m^{(n)} \cos a_m(x+a) \cos \xi_m(y+d) & \text{for } -d \leq y < 0 \\ -\frac{\epsilon_2}{\epsilon_1} \sum_{m=0}^{\infty} q_m^{(n)} \xi_m \sin(\xi_m d) [H_m(x, y) + R_m^H(x, y)] & \text{for } y \geq 0 \end{cases} \quad (4)$$

$$T_E^{(n)}(x, y) = \begin{cases} \sum_{m=1}^{\infty} p_m^{(n)} \sin a_m(x+a) \sin \xi_m(y+d) & \text{for } -d \leq y < 0 \\ \sum_{m=1}^{\infty} p_m^{(n)} \sin(\xi_m d) [E_m(x, y) + R_m^E(x, y)] & \text{for } y \geq 0 \end{cases} \quad (5)$$

$$H_m(x, y) = \frac{e^{i\eta_m y}}{i\eta_m} \cos a_m(x+a) \quad (6)$$

$$E_m(x, y) = e^{i\eta_m y} \sin a_m(x+a) \quad (7)$$

$$R_m^H(x, y) = \int_0^{\infty} \left[H_m(\bar{r}'_1) \frac{\partial G_A^{yy}(\bar{r}, \bar{r}'_1)}{\partial x} - H_m(\bar{r}'_2) \frac{\partial G_A^{yy}(\bar{r}, \bar{r}'_2)}{\partial x} \right] dy' \quad (8)$$

$$R_m^E(x, y) = \int_0^{\infty} \left[G_A^{zz}(\bar{r}, \bar{r}'_1) \frac{\partial E_m(\bar{r}'_1)}{\partial x'} - G_A^{zz}(\bar{r}, \bar{r}'_2) \frac{\partial E_m(\bar{r}'_2)}{\partial x'} \right] dy', \quad (9)$$

$\bar{r}'_1 = (-a, y')$, $\bar{r}'_2 = (a, y')$, and $G_A^{yy,zz}(\bar{r}, \bar{r}')$ are the vector potential Green's functions for the y - and z -directed currents. The unknown modal coefficients, $q_m^{(n)}$ and $p_m^{(n)}$, are defined for the TM (H_z) and TE (E_z) fields for the n th single RG which are rigorously formulated in [6, 7], respectively.

Matching the tangential magnetic fields at $y = 0$, we can determine the unknown modal coefficients of multiple RG, $q_m^{(n)}$ and $p_m^{(n)}$ for the H_z and E_z fields [6, 7], where m and n indicate the m th modal index for the n th RG in Figure 1, and m, n are used for modal expansion and superposition of RG, respectively. It should be noted that the scattered fields, $T_H^{(n)}(x, y)$ and $T_E^{(n)}(x, y)$ in (3), include the unknown modal coefficients, $q_m^{(n)}$ and $p_m^{(n)}$, in terms of modal expansion method [6, 7]. However, the geometry in Figure 1 produces semi-infinite periodic RG ($n = 1, 2, 3, \dots$) and then it results in semi-infinite number of unknown modal coefficients, $q_m^{(n)}$ and $p_m^{(n)}$. Therefore, it is difficult to obtain the modal coefficients, $q_m^{(n)}$ and $p_m^{(n)}$, rigorously. In this work, we use the observation that the fields, $T_H^{(n)}(x, y)$ and $T_E^{(n)}(x, y)$, become those of infinite periodic RG as the index n in Figure 1 increases ($n \rightarrow \infty$) [7]. When the index n is large enough, we can replace the modal coefficients of multiple RG, $q_m^{(n)}$ and $p_m^{(n)}$, with those of infinite periodic RG, q_m^∞ and p_m^∞ , which may be easily obtained by the Floquet modal expansion [6, 7]. This means that subtracting $q_m^\infty e^{i(n-1)k_2 T \sin \theta_i}$ and $p_m^\infty e^{i(n-1)k_2 T \sin \theta_i}$ from $q_m^{(n)}$ and $p_m^{(n)}$ makes the difference of modal coefficients converge to zero [7] when $n \rightarrow \infty$, whereas $\lim_{n \rightarrow \infty} q_m^{(n)}$ and $\lim_{n \rightarrow \infty} p_m^{(n)}$ oscillates. Based on the method in [7], we will derive the simultaneous equations for the TE

modal coefficients $p_m^{(n)}$ of semi-infinite periodic grooves. Multiplying the H_x field continuity at $y = 0$ by $\sin a_l [x - (p - 1)T + a]$ ($l = 1, 2, \dots$ and $p = 1, 2, \dots$) and integrating over $(p - 1)T - a \leq x \leq (p - 1)T + a$ yields the full-wave simultaneous equations for $p_m^{(n)}$ as

$$\sum_{n=1}^{\infty} \sum_{m=1}^{\infty} p_m^{(n)} \psi_{ml}^{(n)} = v_i \cdot s_{E,l}^{(p)}, \quad (10)$$

where l, p are used for mode-matching procedure such as the l th modal index for the p th RG in Figure 1, δ_{ml} is the Kronecker delta,

$$\begin{aligned} \psi_{ml}^{(n)} = & \frac{1}{\mu_1} \xi_m \cos(\xi_m d) a \delta_{np} \delta_{ml} \\ & - \frac{1}{\mu_2} \sin(\xi_m d) [i \eta_m a \delta_{np} \delta_{ml} + I_{ml}^E [(p - n)T]] \end{aligned} \quad (11)$$

$$I_{ml}^E(x_0) = \int_{x_0-a}^{x_0+a} \left. \frac{\partial R_m^E(x, y)}{\partial y} \right|_{y=0} \sin a_l (x - x_0 + a) dx \quad (12)$$

$$s_{E,l}^{(p)} = - \frac{i 2 k_2 \cos \theta_i}{\mu_2} F_l(k_2 \sin \theta_i) e^{i(p-1)k_2 T \sin \theta_i} \quad (13)$$

$$F_m(\xi) = \frac{a_m [(-1)^m e^{i\xi a} - e^{-i\xi a}]}{\xi^2 - a_m^2}. \quad (14)$$

To utilize the subtraction technique with infinite periodic solutions for the geometry in Figure 1, we need to choose a groove index N_G . The groove index means that when $n > N_G$, scattering behaviors of a semi-infinite array are very similar to those of an infinite periodic array and thus we can replace $p_m^{(n)}$ in (10) with p_m^∞ obtained with the Floquet analysis. Therefore, for $n > N_G$, we assume that $p_m^{(n)}$ is almost identical to that of infinite periodic RG p_m^∞ . Utilizing the Floquet theorem [6, 7], $p_m^{(n)} \approx p_m^\infty \exp[i(n - 1)k_2 T \sin \theta_i]$, we get the simplified equations as

$$\sum_{n=1}^{N_G} \sum_{m=1}^{\infty} p_m^{(n)} \psi_{ml}^{(n)} \approx v_i \cdot s_{E,l}^{(p)} - \frac{k_2 a_l}{\pi \mu_2} \sum_{m=1}^{\infty} p_m^\infty a_m \psi_{ml}^\infty, \quad (15)$$

where $1 \leq p \leq N_G$, p_m^∞ should be determined in advance,

$$\psi_{ml}^\infty = \sin(\xi_m d) e^{-i k_2 T \sin \theta_i} \int_0^\infty \frac{(1 + 2v_i) \eta^2 g_{ml}^\infty(-\xi)}{\xi(\xi^2 - a_m^2)(\xi^2 - a_l^2)} dv \quad (16)$$

$$g_{ml}^\infty(\xi) = \left[(-1)^m e^{-i 2 \xi a} + (-1)^l e^{i 2 \xi a} - (-1)^{m+l} - 1 \right] \frac{e^{i[p\xi T + (N_G+1)\phi_0]}}{1 - e^{i\phi_0}}, \quad (17)$$

$\eta = k_2 v(v - i)$, $\xi = \sqrt{k_2^2 - \eta^2}$, and $\phi_0 = (k_2 \sin \theta_i - \xi)T$. The integrand in (16) decreases exponentially with the increase of v and it does not have any singularities with respect to v , thus indicating that our solution (15) is very efficient for numerical computations. Similarly, enforcing the H_z field continuity at $y = 0$ yields the simultaneous equations for the TM modal coefficients $q_m^{(n)}$ which are already obtained in [7]. For reader's convenience, we write the final equations as

$$\sum_{n=1}^{N_G} \sum_{m=0}^{\infty} q_m^{(n)} \phi_{ml}^{(n)} \approx u_i \cdot s_{H,l}^{(p)} - \frac{k_2 \varepsilon_2}{\pi \varepsilon_1} \sum_{m=0}^{\infty} q_m^{\infty} \xi_m \phi_{ml}^{\infty}, \quad (18)$$

where $\alpha_m = 1 + \delta_{m0}$,

$$\begin{aligned} \phi_{ml}^{(n)} &= \cos(\xi_m d) a \alpha_m \delta_{np} \delta_{ml} \\ &+ \frac{\varepsilon_2}{\varepsilon_1} \xi_m \sin(\xi_m d) \left[\frac{a \alpha_m \delta_{np} \delta_{ml}}{i \eta_m} + I_{ml}^H [(p - n)T] \right] \end{aligned} \quad (19)$$

$$\phi_{ml}^{\infty} = \sin(\xi_m d) e^{-ik_2 T \sin \theta_i} \int_0^{\infty} \frac{(1 + 2vi) \xi g_{ml}^{\infty}(-\xi)}{(\xi^2 - a_m^2)(\xi^2 - a_l^2)} dv \quad (20)$$

$$I_{ml}^H(x_0) = \int_{x_0 - a}^{x_0 + a} R_m^H(x, 0) \cos a_l(x - x_0 + a) dx \quad (21)$$

$$s_{H,l}^{(p)} = 2G_l(k_2 \sin \theta_i) e^{i(p-1)k_2 T \sin \theta_i} \quad (22)$$

$$G_m(\xi) = \frac{i\xi [e^{-i\xi a} - (-1)^m e^{i\xi a}]}{\xi^2 - a_m^2}. \quad (23)$$

Even though the simultaneous equations, (15) and (18), are approximate, we can improve the numerical accuracy by increasing a groove index N_G in (15) and (18).

Summing all far-fields of semi-infinite periodic RG, we asymptotically write the scattered electric fields ($y > 0$) as

$$\bar{E}^{tot}(\rho, \theta; \theta_i) = \hat{\phi} u_i \eta_2 H_z(\rho, \theta) + \hat{z} v_i E_z(\rho, \theta), \quad (24)$$

where $\rho \rightarrow \infty$, $\theta = \tan^{-1}(x/y)$, $\phi_f = k_2 T(\sin \theta_i - \sin \theta)$,

$$\begin{aligned} H_z(\rho, \theta) \approx & \frac{e^{i(k_2 \rho + \pi/4)}}{\sqrt{2\pi k_2 \rho}} \frac{\varepsilon_2}{\varepsilon_1} \sum_{m=0}^{\infty} \left\{ \sum_{n=1}^{N_G} q_m^{(n)} e^{-i(n-1)k_2 T \sin \theta} + q_m^{\infty} \frac{e^{-i\phi_f/2}}{\sin(\phi_f/2)} \right. \\ & \left. \left[\frac{i}{2} - e^{iN_G \phi_f/2} \sin(N_G \phi_f/2) \right] \right\} \xi_m \sin(\xi_m d) G_m(-k_2 \sin \theta) + \frac{1}{2} H_z^{pw}(\rho, \theta) \end{aligned} \quad (25)$$

$$E_z(\rho, \theta) \approx \frac{e^{i(k_2\rho - \pi/4)}}{\sqrt{2\pi k_2\rho}} k_2 \cos\theta \sum_{m=1}^{\infty} \left\{ \sum_{n=1}^{N_G} p_m^{(n)} e^{-i(n-1)k_2 T \sin\theta} + p_m^{\infty} \frac{e^{-i\phi_f/2}}{\sin(\phi_f/2)} \right. \\ \left. \left[\frac{i}{2} - e^{iN_G\phi_f/2} \sin(N_G\phi_f/2) \right] \right\} \sin(\xi_m d) F_m(-k_2 \sin\theta) + \frac{1}{2} E_z^{pw}(\rho, \theta), \quad (26)$$

and $H_z^{pw}(\rho, \theta)$, $E_z^{pw}(\rho, \theta)$ are far-fields of infinite periodic RG which can be obtained with the Floquet modes. In a dominant-mode approximation ($M = 1$ and $N_G = 1$), (24) for semi-infinite periodic RG is simplified as

$$\bar{E}^{tot}(\rho, \theta; \theta_i) \approx \frac{e^{i(k_2\rho - \pi/4)}}{\sqrt{2\pi k_2\rho}} 2i \left\{ \frac{\varepsilon_2}{\varepsilon_1} 4k_1 a^2 \sin(k_1 d) \cdot \text{Sa}(k_2 a \sin\theta_i) \right. \\ \times \frac{\text{Sa}(k_2 a \sin\theta)}{\phi_1} \left[\frac{\phi_1 - \phi_2}{\phi_3} + \frac{ie^{-i\phi_f/2}}{2 \sin(\phi_f/2)} - 1 \right] u_i \hat{\phi} \\ - k_2^2 \sin(\xi_1 d) \cos\theta_i \cdot F_1(k_2 \sin\theta_i) \frac{\cos\theta \cdot F_1(k_2 \sin\theta)}{\psi_1} \\ \left. \times \left[\frac{\psi_1 - \psi_2}{\psi_3} + \frac{ie^{-i\phi_f/2}}{2 \sin(\phi_f/2)} - 1 \right] v_i \hat{z} \right\}, \quad (27)$$

where M denotes the number of truncated modes in region (I) ($y < 0$), $\text{Sa}(x) = \sin x/x$,

$$\phi_1 = 2a \cos(k_1 d) + \frac{\varepsilon_2}{\varepsilon_1} k_1 \sin(k_1 d) \\ \times \left\{ \frac{2a}{ik_2} + \frac{k_2}{\pi} \int_0^{\infty} \frac{1 + 2vi}{\xi^3} [f_+^H(\xi) + f_-^H(\xi)]_{m=l=0} dv \right\} \quad (28)$$

$$\phi_2 = \frac{\varepsilon_2}{\varepsilon_1} \frac{2k_1 k_2}{\pi} \sin(k_1 d) \int_0^{\infty} \frac{1 + 2vi}{\xi^3} \frac{[\cos(2\xi a) - 1] e^{i(\xi + k_2 \sin\theta_i)T}}{1 - e^{i(\xi + k_2 \sin\theta_i)T}} dv \quad (29)$$

$$\phi_3 = 2a \cos(k_1 d) + \frac{\varepsilon_2}{\varepsilon_1} k_1 \sin(k_1 d) \\ \times \left\{ \frac{2a}{ik_2} + \frac{2k_2}{\pi} \int_0^{\infty} \frac{1 + 2vi}{\xi^3} (e^{i2\xi a} - 1) dv \right\} \quad (30)$$

$$\psi_1 = \frac{\mu_2}{\mu_1} \xi_1 a \cos(\xi_1 d) - \sin(\xi_1 d) \\ \times \left\{ i\eta_1 a - \frac{k_2 a_1^2}{\pi} \int_0^{\infty} \frac{\eta^2(1 + 2vi)}{\xi(\xi^2 - a_1^2)^2} [f_+^H(\xi) + f_-^H(\xi)]_{m=l=1} dv \right\} \quad (31)$$

$$\psi_2 = -\frac{2k_2 a_1^2}{\pi} \sin(\xi_1 d) \int_0^{\infty} \frac{\eta^2(1 + 2vi)}{\xi(\xi^2 - a_1^2)^2} \frac{[\cos(2\xi a) + 1] e^{i(\xi + k_2 \sin\theta_i)T}}{1 - e^{i(\xi + k_2 \sin\theta_i)T}} dv \quad (32)$$

$$\psi_3 = \frac{\mu_2}{\mu_1} \xi_1 a \cos(\xi_1 d) - \sin(\xi_1 d) \times \left\{ i\eta_1 a + \frac{2k_2 a_1^2}{\pi} \int_0^\infty \frac{\eta^2(1+2v_i)}{\xi(\xi^2 - a_1^2)^2} \left(e^{i2\xi a} + 1 \right) dv \right\} \quad (33)$$

$$f_{\pm}^H(\xi) = \frac{\{e^{i[\xi(T-a) \pm k_2 T \sin \theta_i]} - (-1)^m e^{i\xi a}\}}{1 - e^{i(\xi \pm k_2 \sin \theta_i)T}} \left[(-1)^l e^{-i\xi a} - e^{i\xi a} \right]. \quad (34)$$

The Floquet-modes based plane-wave terms, $H_z^{pw}(\rho, \theta)$ and $E_z^{pw}(\rho, \theta)$, are omitted in (27). When $u_i = 1$ and $v_i = \pm i$, the total scattered electric fields for the circularly polarized plane-wave incidence in the far-field region are represented as

$$\begin{aligned} \bar{E}^{tot}(\rho, \theta; \theta_i) &= \frac{1}{\sqrt{2}} [u_i \eta_2 H_z(\rho, \theta) - i v_i E_z(\rho, \theta)] \hat{C}_R \\ &+ \frac{1}{\sqrt{2}} [u_i \eta_2 H_z(\rho, \theta) + i v_i E_z(\rho, \theta)] \hat{C}_L \end{aligned} \quad (35)$$

where \hat{C}_R and \hat{C}_L denote right-handed (RH) and left-handed (LH) circular polarization (CP) unit vectors, respectively,

3. APPLICATION TO FINITE PERIODIC GROOVES

Although the finite periodic grooves can be rigorously analyzed by (15) and (18) with $q_m^\infty = p_m^\infty = 0$ [6, 7], the formulations, (15) and (18), are inefficient and time-consuming when $N \gg 1$ (N : the number of finite grooves). Once we obtain the diffracted fields of semi-infinite periodic grooves, we can approximately but efficiently calculate those of finite periodic grooves with the summation of two semi-infinite periodic grooves. The basic concept is illustrated in Figure 3. The

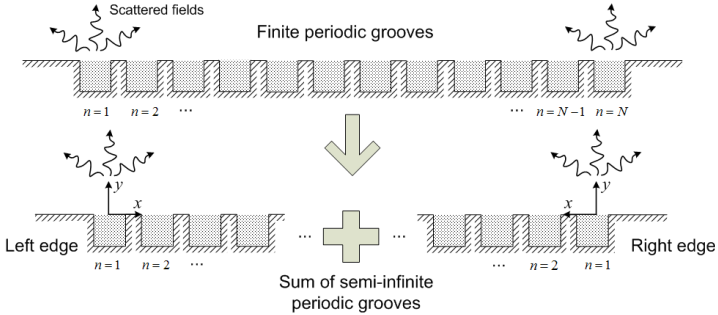


Figure 3. Interpretation of scattering by finite periodic grooves in terms of the summation of semi-infinite periodic grooves.

edge diffracted field is one of fundamental and important factors of the GTD (Geometrical Theory of Diffraction) or UTD (Uniform Theory of Diffraction). In the GTD, the summation of edge diffracted fields can result in the approximate diffracted fields of a real structure. We can adopt the similar method used in the GTD for finite periodic gratings to obtain those of large gratings.

In our method, the diffracted fields (24) are similarly used as the edge diffracted fields in the GTD. Combining (24) and corresponding translational phases, we can obtain the diffraction solutions for actual finite periodic gratings with numerous elements ($N \gg 1$) as

$$\bar{E}^{\text{finite}}(\rho, \theta) \approx \lim_{\rho \rightarrow \infty} \left[e^{-ik_2 x_l \sin \theta} \bar{E}^{\text{left}}(\rho, \theta; \theta_i) + e^{-ik_2 x_r \sin \theta} \bar{E}^{\text{right}}(\rho, \theta; \theta_i) \right], \quad (36)$$

where x_l and x_r are the positions of left and right semi-infinite periodic grooves in the x -axis,

$$\bar{E}^{\text{left}}(\rho, \theta; \theta_i) = \bar{E}^{\text{tot}}(x, y) = \bar{E}^{\text{tot}}(\rho, \theta; \theta_i) \quad (37)$$

$$\bar{E}^{\text{right}}(\rho, \theta; \theta_i) = \bar{E}^{\text{tot}}(-x, y) = \bar{E}^{\text{tot}}(\rho, -\theta; -\theta_i). \quad (38)$$

When the number of finite grooves is N , we may set $x_l = 0$ and $x_r = (N - 1)T$ for (36).

4. NUMERICAL COMPUTATIONS

Figure 4 illustrates the behaviors of scattered electric fields of semi-infinite periodic RG for RHCP incidence ($u_i = 1$ and $v_i = i$). The scattered electric field [dB] is defined by $20 \log_{10} |2\bar{E}^{\text{tot}}(\rho, \theta)/H_0^{(1)}(k_2 \rho)|$, where $H_0^{(1)}(\cdot)$ is the zeroth order Hankel function of the first kind. As a period T increases, maximum cross-polarization ratio for LHCP and RHCP tends to increase. The Floquet-mode related peaks also vary with the change of T . Figure 5 shows the scattered electric fields behaviors of large number of multiple RG [6] for the TE plane-wave incidence ($u_i = 0$ and $v_i = 1$). The total width of finite periodic gratings used for numerical computation is almost $1500\lambda_0$. The analytic simulations for multiple RG ($N = 1000$) were performed with the method in [6]. These analytic scattering behaviors are compared with the combined equations based on semi-infinite periodic RG shown in (36). Overall diffraction tendency in Figure 5 resembles each other, thus confirming that an approximate equation based on semi-infinite periodic RG (36) can be utilized to predict the scattered fields of actual finite gratings. It should be also noted that a dominant mode solution (27) agrees well with the full-wave calculations. In our computations, the required matrix size for

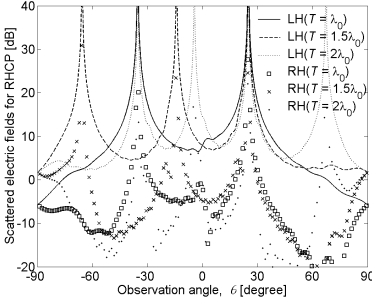


Figure 4. Behaviors of scattered electric fields of semi-infinite periodic rectangular grooves for RHCP incidence with $u_i = 1$, $v_i = i$, $a = 0.25\lambda_0$, $d = 0.6\lambda_0$, $\varepsilon_1 = \varepsilon_2 = \varepsilon_0$, $\mu_1 = \mu_2 = \mu_0$, $\theta_i = 25^\circ$, $N_G = 10$, and $M = 4$.

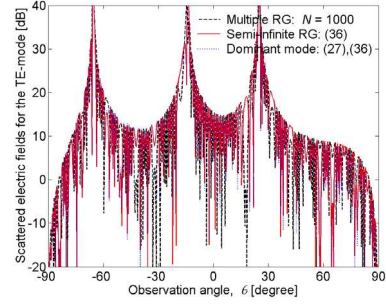


Figure 5. Scattered electric fields for large number of rectangular grooves (RG) versus an observation angle θ with $u_i = 0$, $v_i = 1$, $T = 1.5\lambda_0$ and the same parameters in Figure 4.

multiple RG is $N \cdot M$ ($= 4000$), whereas that for (36) is only $N_G \cdot M$ ($= 40$). The parameters, N , N_G , and M , denote the numbers of actual periodic gratings, RG necessary to formulate the semi-infinite periodic RG, and truncated modal coefficients for each RG, respectively.

5. CONCLUSION

Using an overlapping T-block method and the subtraction technique with infinite periodic solutions, we approximately derived the solutions of semi-infinite periodic RG in a perfectly conducting plane. Our solutions for semi-infinite periodic RG were, then, combined to estimate the diffraction characteristics of finite periodic gratings with numerous diffracting elements. We numerically proved that the approximate solutions based on semi-infinite periodic grooves well predict the diffracted fields of large finite gratings.

REFERENCES

1. Bendickson, J. M., E. N. Glytsis, T. K. Gaylord, and D. L. Brundrett, "Guided-mode resonant subwavelength gratings: Effects of finite beams and finite gratings," *J. Opt. Soc. Am. A*, Vol. 18, No. 6, 1912–1928, 2001.

2. Wu, S.-D. and E. N. Glytsis, "Finite-number-of-periods holographic gratings with finite-width incident beams: Analysis using the finite-difference frequency-domain method," *J. Opt. Soc. Am. A*, Vol. 19, No. 10, 2018–2029, 2002.
3. Lin, A. and J. Phillips, "Optimization of random diffraction gratings in thin-film solar cells using genetic algorithms," *Sol. Energ. Mat. Sol. C*, Vol. 92, No. 12, 1689–1696, 2008.
4. Basha, M. A., S. K. Chaudhuri, S. Safavi-Naeini, and H. J. Eom, "Rigorous formulation for electromagnetic plane-wave scattering from a general-shaped groove in a perfectly conducting plane," *J. Opt. Soc. Am. A*, Vol. 24, No. 6, 1647–1655, 2007.
5. Scharstein, R. W., J. M. Keen, and D. L. Faircloth, "Two-term Ritz-Galerkin solution for the low frequency scattering by a rectangular trough in a soft ground plane," *IEEE Trans. Antennas Propagat.*, Vol. 56, No. 7, 1993–2001, 2008.
6. Cho, Y. H., "TE scattering from large number of grooves using Green's functions and Floquet modes," *2007 Korea-Japan Micro. Wave Conference (KJMW)*, 41–44, 2007.
7. Cho, Y. H., "Transverse magnetic plane-wave scattering equations for infinite and semi-infinite rectangular grooves in a conducting plane," *IET Proc. — Microw. Antennas Propag.*, Vol. 2, No. 7, 704–710, 2008.
8. Linton, C. M. and P. A. Martin, "Semi-infinite arrays of isotropic point scatters. A unified approach," *SIAM J. Appl. Math.*, Vol. 64, No. 3, 1035–1056, 2004.
9. Linton, C. M., R. Porter, and I. Thompson, "Scattering by a semi-infinite periodic array and the excitation of surface waves," *SIAM J. Appl. Math.*, Vol. 67, No. 5, 1233–1258, 2007.
10. Citrin, D. S., Y. Wang, and Z. Zhou, "Far-field optical coupling to semi-infinite metal-nanoparticle chains," *J. Opt. Soc. Am. B*, Vol. 25, No. 6, 937–944, 2008.
11. Wasyliwskyj, W., "Mutual coupling effects in semi-infinite arrays," *IEEE Trans. Antennas Propagat.*, Vol. 21, No. 3, 277–285, 1973.
12. Fallahi, A. and C. Hafner, "Analysis of semi-infinite periodic structures using a domain reduction technique," *J. Opt. Soc. Am. A*, Vol. 27, No. 1, 40–49, 2010.
13. Hills, N. L. and S. N. Karp, "Semi-infinite diffraction gratings — I," *Comm. Pure Appl. Math.*, Vol. 18, No. 1–2, 203–233, 1965.
14. Zheng, J.-P. and K. Kobayashi, "Diffraction by a semi-infinite parallel-plate waveguide with sinusoidal wall corrugation:

- Combined perturbation and Wiener-Hopf analysis,” *Progress In Electromagnetics Research B*, Vol. 13, 75–110, 2009.
15. Skinner, J. P. and P. J. Collins, “A one-sided version of the Poisson sum formula for semi-infinite array Green’s functions,” *IEEE Trans. Antennas Propagat.*, Vol. 45, No. 4, 601–607, Apr. 1997.
 16. Capolino, F., M. Albani, S. Maci, and L. B. Felsen, “Frequency-domain Green’s function for a planar periodic semi-infinite phased array — Part I: Truncated Floquet wave formulation,” *IEEE Trans. Antennas Propagat.*, Vol. 48, No. 1, 67–74, Jan. 2000.
 17. Polemi, A., A. Toccafondi, and S. Maci, “High-frequency Green’s function for a semi-infinite array of electric dipoles on a grounded slab — Part I: Formulation,” *IEEE Trans. Antennas Propagat.*, Vol. 49, No. 12, 1667–1677, Dec. 2001.